


Article

Effect of Phosphorylation Sites Mutations on the Subcellular Localization and Activity of AGPase Bt2 Subunit: Implications for Improved Starch Biosynthesis in Maize

Guowu Yu ^{1,2,*}, Noman Shoaib ^{3,4,†} , Yang Yang ^{1,2}, Lun Liu ^{1,2}, Nishbah Mughal ^{1,2}, Yuewei Mou ^{1,2} and Yubi Huang ^{1,2}

¹ State Key Laboratory of Crop Gene Exploration and Utilization in Southwest China, Sichuan Agricultural University, Chengdu 611130, China; 2019301069@stu.sicau.edu.cn (Y.Y.); liulun@stu.sicau.edu.cn (L.L.); 2020601004@stu.sicau.edu.cn (N.M.); mouyuewei@stu.sicau.edu.cn (Y.M.); 10024@sicau.edu.cn (Y.H.)

² National Demonstration Center for Experimental Crop Science Education, College of Agronomy, Sichuan Agricultural University, Chengdu 611130, China

³ CAS Key Laboratory of Mountain Ecological Restoration and Bioresource Utilization, Ecological Restoration Biodiversity Conservation Key Laboratory of Sichuan Province, Chengdu Institute of Biology, Chinese Academy of Sciences, Chengdu 610041, China; noman@cib.ac.cn

⁴ University of Chinese Academy of Sciences, Beijing 101408, China

* Correspondence: 13862@sicau.edu.cn

† These authors contributed equally to this work.

Abstract: ADP-Glc pyrophosphorylase (AGPase) is a pivotal enzyme catalyzing the conversion of ATP and glucose-1-phosphate (Glc-1-P) to adenosine diphosphate glucose (ADP-Glc), thereby serving as a rate-limiting factor in starch biosynthesis in crops. Although previous investigations have suggested phosphorylation-based regulation of AGPase in maize, the explicit modulation mechanisms have yet to be elucidated. This research evaluated the effect of point mutations at phosphorylation sites (identified using iTRAQTM AB SCIEX, Framingham, MA, USA) on the subcellular localization and activity of the AGPase small subunit Bt2, and its interaction with the large subunit Sh2, in maize. Despite the induction of point mutations, subcellular localization of the Bt2 subunit remained unaltered, primarily within the cytoplasm and nucleus. The interaction between Bt2 and Sh2 subunits continued, mainly in the chloroplast. Notably, an increase in AGPase activity was observed in the case of simulated phosphorylation point mutations, whereas dephosphorylation activity significantly diminished relative to the wild type. These findings demonstrate that point mutations do not affect the subcellular localization of the Bt2 subunit or its interaction with the Sh2 subunit, but substantially modulate AGPase activity. This study provides critical insights into the role of point mutations in enhancing AGPase activity, thus potentially accelerating the production of ADP-Glc, the primary substrate for starch synthesis, promising implications for improved starch biosynthesis in maize.

Keywords: AGPase; enzyme activity regulation; AGPase phosphorylation; subcellular localization of AGPase



Citation: Yu, G.; Shoaib, N.; Yang, Y.; Liu, L.; Mughal, N.; Mou, Y.; Huang, Y. Effect of Phosphorylation Sites Mutations on the Subcellular Localization and Activity of AGPase Bt2 Subunit: Implications for Improved Starch Biosynthesis in Maize. *Agronomy* **2023**, *13*, 2119. <https://doi.org/10.3390/agronomy13082119>

Academic Editors: Eszter Virag and Szilvia Veres

Received: 25 July 2023

Revised: 6 August 2023

Accepted: 8 August 2023

Published: 13 August 2023



Copyright: © 2023 by the authors. Licensee MDPI, Basel, Switzerland. This article is an open access article distributed under the terms and conditions of the Creative Commons Attribution (CC BY) license (<https://creativecommons.org/licenses/by/4.0/>).

1. Introduction

Starch, recognized for its environmentally friendly properties, widespread availability, cost-effectiveness, and ease of modification, acts as a fundamental raw material across a variety of industries including food, medicine, bioethanol production, biodegradable materials, and ecofriendly water treatment agents [1–3]. Given the ongoing resource scarcity per capita and increasing emphasis on environmental preservation in China, corn starch has risen to prominence due to its high yield [4] and adaptability in both primary and secondary product processing [5]. Consequently, investigations into corn starch synthesis and the development of methodologies to enhance starch production have become increasingly

crucial. The complex process of starch biosynthesis fundamentally relies on a sequence of catalytic enzymes, including adenosine diphosphate glucose pyrophosphorylase (AGPase), starch synthase (SS), starch branching enzyme (SBE), and starch debranching enzyme (DBE) [6]. Of these, AGPase holds a crucial position as a rate-determining enzyme in starch biosynthesis and catalyzes the conversion of ATP and glucose-1-phosphate (Glc-1-P) to adenosine diphosphate glucose (ADP-Glc). This reaction is considered the first committed step in starch synthesis. Since this is an early step and its product, ADP-Glc, is the primary substrate for the subsequent starch production (act as a substrate to extend the α -1,4 linked glucans by SS [7], the rate at which this reaction occurs can effectively control the overall rate of starch synthesis. In addition, there are indications that AGPase does not entirely involve in starch biosynthesis, as it requires a primer of reasonable chain length [8]. Based on biochemical evidence, it is assumed that starch phosphorylase (SP) is involved in the initiation and amplification starch biosynthesis in plants [9,10]. There are two possible routes for starch synthesis: either through the PHO1 or AGPase/SS, which depend on the availability of substrate-level Glc-1-P [11,12].

In higher plants, AGPase manifests as a heterotetramer composed of two small and two large subunits (α 2 β 2). While the proteins encoded by these subunits bear resemblance, they present key distinctions. The small subunit, for example, demonstrates a higher level of conservation (85–95%) compared to the large subunit (50–60%). Moreover, the molecular weight of the large subunit (54–60 kDa) slightly exceeds that of the small subunit (51–55 kDa) [13]. The efficient activity of AGPase relies on the synergistic interaction between these two subunits [14]. The large subunit functions as the regulatory entity modulating metabolic activity, while the small subunit assumes the role of the catalyst facilitating its metabolic operation [15]. This division of roles within the heterotetrameric structure of AGPase underscores its intricate function in starch biosynthesis. In many species, AGPase primarily occupies the plastids, with plastid-located AGPase serving as the sole source of ADP-Glc, a precursor integral to starch synthesis. However, in grain endosperms, the majority of ADP-Glc is derived from AGPase located in the cytoplasm. Therefore, in grain endosperm, AGPase is found both in the cytoplasm and plastids, with a significant majority (85–95%) of its activity transpiring in the cytoplasm [16]. These findings suggest a unique pathway in cereal endosperm starch synthesis that requires an ADP-Glc transporter to shuttle ADP-Glc, generated by cytoplasmic AGPase, into the plastids [17,18].

The regulation of AGPase, which varies across tissues and cells, profoundly influences its activity. Its function is comodulated via diverse regulatory mechanisms, encompassing redox [19], allosteric [20], and transcriptional approaches [21,22]. With the progression of experimental methodologies, notably mass spectrometry and affinity chromatography, comprehension of proteomes and phosphoproteomes has been significantly extended. Previous research has identified phosphorylated AGPase in a variety of species and tissues [23,24]. In particular, grain-focused studies have indicated the occurrence of AGPase subunit phosphorylation. For instance, differential gel electrophoresis analysis of grown wheat seeds inferred that the small subunit of plastid AGPase undergoes phosphorylation, although the specific site of phosphorylation remained unidentified [25]. Previous experiments in our laboratory suggest that when samples underwent alkaline phosphatase treatment for gel activity measurement, the resulting enzymatic activity was less compared to the phosphorylated control, insinuating an interrelationship between AGPase activity and phosphorylation [26]. More recently, research has verified the phosphorylation of the AGPase subunit in the wheat endosperm [27], with *in vitro* trials involving recombinant AGPase from wheat endosperm and calcium-dependent protein kinase indicating that phosphorylation emerges in both of the subunits.

In this study, the phosphorylation and dephosphorylation states were emulated through point mutation at the three sites identified using mass spectrometry: Bt2-S10, Bt2-T451, and Bt2-T462. To simulate dephosphorylation, all three sites were concurrently mutated to alanine (A). Similarly, a collective mutation to glutamic acid (E) was conducted to imitate phosphorylation [26]. A central question under investigation was whether these

mutations would alter the subcellular localization, interaction with the large subunit, and AGPase activity. Our findings established that the mutations at S10/T451/T462 (A/E) did not bring about any alterations in the subcellular localization of Bt2 nor did they affect its interaction with Sh2. Notably, however, the mutations that simulated phosphorylation increased AGPase activity. These results, therefore, suggest that phosphorylation could also serve as a mechanism for the regulation of AGPase activity during starch biosynthesis.

2. Materials and Methods

2.1. Preparation of Experiment Materials

The maize variety Mo17 utilized in this study was kindly provided by the College of Agriculture, Sichuan Agricultural University. The maize was cultivated at the Chongzhou Base, with endosperm protoplasts isolated 6–7 days after pollination (DAP). Etiolated seedlings were initially grown in a controlled environment at 28 °C, with a light–dark cycle of 16 h light and 8 h dark. After a germination period of three days, the seedlings were transferred to dark conditions for continued cultivation. The yeast strain Y2H was maintained in-house. The subcellular localization vector pCAMBIA2300-35S-eGFP, yeast vectors pGADT7 and pGBKT7, bimolecular fluorescence complementation vectors E2913 (pSAT6-nEYFP-N1 for linking to Bt2) and E3086 (pSAT6-cEYFP-N1 for linking to Sh2), as well as the transient expression vectors pBI221-ubiquitin-GUS, were also available in Yu's laboratory.

2.2. iTRAQTM Labeling and Mass Spectrometry Analysis

The iTRAQTM method [28] was utilized to identify phosphorylated proteins in this study. Three samples of Mo17 corn 25 DAP grain protein were collected during both day- and night-time, and the experiment was repeated. To begin, sample lysis and protein extraction were performed using an SDT buffer consisting of 4% SDS, 100 mM Tris-HCl, and 1 mM DTT at pH 7.6. The concentration of the extracted proteins was determined using the BCA Protein Assay Kit from Bio-Rad, Hercules, CA, USA. Protein digestion was carried out using trypsin following the filter-aided sample preparation (FASP) procedure. The resulting digested peptides from each sample were desalted using C18 Cartridges (EmporeTM SPE Cartridges C18, standard density), concentrated through vacuum centrifugation, and reconstituted in 40 µL of 0.1% (*v/v*) formic acid. The phosphopeptides were then enriched using the High-SelectTM Fe-NTA Phosphopeptides Enrichment Kit, according to the manufacturer's instructions (Thermo Scientific, Hanover Park, IL, USA). The phosphopeptides were lyophilized and subsequently resuspended in 20 µL of loading buffer (0.1% formic acid). For LC-MS analysis, a timsTOF Pro mass spectrometer (Bruker, Billerica, MA, USA) coupled with Nanoelute (Bruker Daltonics) was employed for a total duration of 60 min. The peptides were loaded onto a C18-reversed phase analytical column (25 cm long, 75 µm inner diameter, 1.9 µm, C18), and separation was achieved using a linear gradient of buffer B (84% acetonitrile and 0.1% formic acid) at a flow rate of 300 g/min, with buffer A (0.1% formic acid) as the starting buffer. The mass spectrometer operated in positive ion mode, collecting ion mobility MS spectra within the mass range of *m/z* 100–1700 and 1/*k*₀ values ranging from 0.6 to 1.6. Following this, 10 cycles of PASEF MS/MS were performed with a target intensity of 1.5 k and a threshold of 2500. The active exclusion was enabled with a release time of 0.4 min.

The original data obtained from the mass spectrometry analysis were in RAW file format. For library identification and quantitative analysis, MaxQuant software (version 1.5.3.17) was utilized.

2.3. Site-Directed Point Mutations

Site-specific primers for gene mutations Bt2-S10A-F/R, Bt2-S10E-F/R, Bt2-T451A-F/R, Bt2-T451E-F/R, Bt2-T462A-F/R, and Bt2-T462E-F/R were designed according to NCBI guidelines, leading to a total of six pairs (primer sequences detailed in Table S1). The positive cloning vector UG221-Bt2, maintained in-house, served as the template plasmid

for mutation. PCR conditions were set as follows: an initial denaturation step at 95 °C for 3 min, followed by 34 cycles of 95 °C for 30 s, 58 °C for 30 s, and 72 °C for 8 min. The PCR protocol concluded with a final extension at 72 °C for 10 min, with products stored at 12 °C. Upon completion of PCR, 1 µL of *DpnI* was directly added to the reaction mixture, stirred, and then incubated at 37 °C for 30 min. Post-*DpnI* digestion, the mixture could be used immediately for transformation or stored at −20 °C for later use. After transformation, single colonies were isolated, cultured, validated, and sent to the company for sequencing. Upon sequencing confirmation, plasmids were extracted and either stored or used for vector replacement.

2.4. Subcellular Localization Analysis

Subcellular localization vectors were constructed for both wild type and mutant type, leading to the creation of 2300-Bt2-eGFP, 2300-Bt2-S10/T451/T462A-eGFP, and 2300-Bt2-S10/T451/T462E-eGFP fusion plasmids as per described in [29]. The selected restriction enzyme sites were *KpnI* and *XbaI*, with homologous recombination primers listed in Supplementary Table S1. Constructed plasmids were introduced into endosperm protoplasts using the polyethylene glycol-calcium (PEG-Ca²⁺) transformation method. Following transformation, protoplasts were cultured for 16 h either in the dark or under low-light conditions. Post-culture, the intracellular distribution of GFP was examined using microscopy.

2.5. Yeast Two-Hybrid Assay

The fusion plasmids pGADT7-Bt2, pGADT7-Bt2-S10/T451/T462A, pGADT7-Bt2-S10/T451/T462E, and pGBKT7-Sh2 were constructed according to [30]. The restriction enzyme sites used were *EcoRI* and *BamHI*, and the homologous recombination primers are presented in Table S1. The combination of pGADT7 and pGBKT7 was utilized as a negative control. The resulting plasmid combinations were introduced into Y2H yeast-competent cells using the PEG/LiAc method. Following the transformation process, the cells were spread onto selection media lacking tryptophan (SD/Trp). The plates were incubated at 28 °C for approximately three days. Positive clones were then selected and cultured in liquid media without two necessary nutrients until reaching an optical density (OD₆₀₀) between 0.5 and 0.8. The yeast culture was then collected, washed with sterile water, and spotted onto both two-deficient and four-deficient solid media at various concentration gradients (10^{−1}, 10^{−2}, 10^{−3}, 10^{−4}, from left to right). The plates were cultured for an additional 2–3 days and the growth of individual yeast colonies was subsequently observed.

2.6. Bimolecular Fluorescence Complementation

The BiFC expression vectors were constructed utilizing E2913 (pSAT6-nEYFP-N1) and E3086 (pSAT6-cEYFP-N1) to harbor the Bt2 (and its mutant forms) and Sh2 genes, respectively. This yielded fusion plasmids E2913-Bt2-N YFP, E2913-Bt2-S10/T451/T462A-N YFP, E2913-Bt2-S10/T451/T462E-N YFP, and E3086-Sh2-C YFP. The restriction enzyme sites selected for this process were *EcoRI* and *SmaI*, and the relevant homologous recombination primers are documented in Table S1. The combination of E2913-N YFP and E3086-C YFP was employed as a negative control. The combined plasmids were introduced into maize leaf etiolated seedling protoplasts using the PEG-Ca²⁺ transformation method. Following a 24 h incubation period in darkness, the YFP yellow fluorescence signal was inspected under a confocal microscope.

2.7. Protoplast Preparation

Seedling-stage leaves exhibiting yellow heads were delicately sliced into 0.5–1 mm wide leaf fillets using a sharp blade. Concurrently, endosperm from maize (7–9 DAP) was carefully removed with precision tweezers and swiftly segmented into minute pieces. To prevent desiccation, these were immersed in an enzyme solution composed of 1.5% cellulase, 0.75% pectin, 10 mM MES, 600 mM mannitol, 10 mM CaCl₂, and 0.1% BSA. The endosperm underwent enzymatic hydrolysis for 4–6 h. Post-hydrolysis, an equal

volume of W5 solution (154 mM NaCl, 125 mM CaCl₂, 5 mM KCl, 2 mM MES-KOH) was added, followed by brief centrifugation at 90× g for 3 min at 4 °C. The supernatant was discarded, protoplasts were resuspended in 5 mL of W5, and the centrifugation step was repeated. The supernatant was subsequently discarded, 1 mL of W5 was added, and the solution was allowed to rest on ice for 30 min. The protoplasts were then resuspended in MMG solution (400 mM mannitol, 15 mM MgCl₂, 4 mM MES-KOH, pH 5.6) at a density of approximately 2 × 10⁵ protoplasts/mL. The transformation process was initiated by adding 10–20 µg of plant expression vector to the protoplast suspension. A gentle mixing followed, succeeded by the addition of 100 µL of PEG-Ca²⁺ solution (4 M mannitol, 10 mM CaCl₂, 40% PEG). The induced transformation was carried out in darkness for 15 min, then halted by adding 400 µL of W5 solution. Following a brief centrifugation at 90× g for 2 min at room temperature and discarding the supernatant, an additional 100 µL of W5 solution was gently mixed in. The protoplasts were incubated in the dark at 28 °C for 12 h and subsequently observed under a microscope. Protoplasts were then gathered via a brief centrifugation at room temperature and a fraction of this was selected for fluorescence signal observation under a confocal microscope.

2.8. Determination of AGPase Activity

To assess the activity of AGPase, the change in RLUC (Renilla luciferase) value corresponding to ATP production was measured using the ADP/ATP luminescence detection kit (Beyotime, Hangzhou, China). Fusion plasmids 221-Bt2, 221-Bt2-S10/T451/T462A, 221-Bt2-S10/T451/T462E, and 221-Sh2 were constructed utilizing *Bam*HI and *Sac*I restriction sites, with the corresponding homologous recombination primers delineated in Table S1. AGPase activity was inferred based on the enzyme's reversible property that facilitates ADPG catalysis to consume Pi and generate ATP. The resultant ATP volume was quantified to assess AGPase activity changes. These constructed plasmids were introduced into the etiolated seedling protoplasts via PEG-Ca²⁺ transformation. Following 24 h of dark cultivation, the ATP levels were determined. For in vitro AGPase activity assessment, an ATP detection kit was employed. After 14–16 h of dark incubation, the protoplasts were harvested via centrifugation at room temperature (90 g, 1 min). RLUC activity was evaluated using the Luciferase Assay System (Promega, Madison, WI, USA), adhering to the instructions outlined in the ATP Assay Kit (Beyotime). GUS activity was assessed by adding 40 µL of cell lysate supernatant to 40 µL of 4-methylumbelliferyl-β-D-glucuronide (MUG) reaction substrate. After thorough mixing, 30 µL of the reaction mixture was halted with 60 µL of 0.3 M Na₂CO₃, and GUS activity was immediately recorded at time zero after sampling 75 µL of the mixture. The remaining 50 µL of the reaction solution was further incubated in the dark at 37 °C for 4 h, then halted with 60 µL of 0.3 M Na₂CO₃. GUS activity was recorded after the complete 4 h incubation period. The halted reaction solution was transferred to a black 96-well cell culture plate, and GUS activity was assessed using a fluorescence spectrophotometer. The ratio of RLUC activity to GUS activity was used as a measure of AGPase activity.

3. Results

3.1. iTRAQTM Identification of Bt2 Phosphorylation Sites

To identify the specific phosphorylation site on Sh2 during starch biosynthesis in maize kernels, endosperm from three different sources, including 15DAP 08-641 maize, transgenic maize, and Mo17 inbred line collected at 25DAP, during the day and night, were subjected to iTRAQ analysis. Our results point toward the phosphorylation of Bt2 at S10, T451, and T462 mentioned in [26]. This finding elucidates that the phosphorylation of Bt2 possibly occurs at S10, T451, and 462 in the maize endosperm.

3.2. Site-Directed Point Mutations

The Bt2 gene spans a total length of 1428 base pairs (bp). Specific mutation primers were engineered, and the resulting sequences were aligned using DNAMAN software

(<https://www.lynnon.com/>). Figure 1 presents the sequence outcomes of the mutation sites following simulated processes of phosphorylation (E) and dephosphorylation (A). These confirmed mutated clones were then used for amplification of the mutated Bt2, paving the way for future recombination with required vectors.

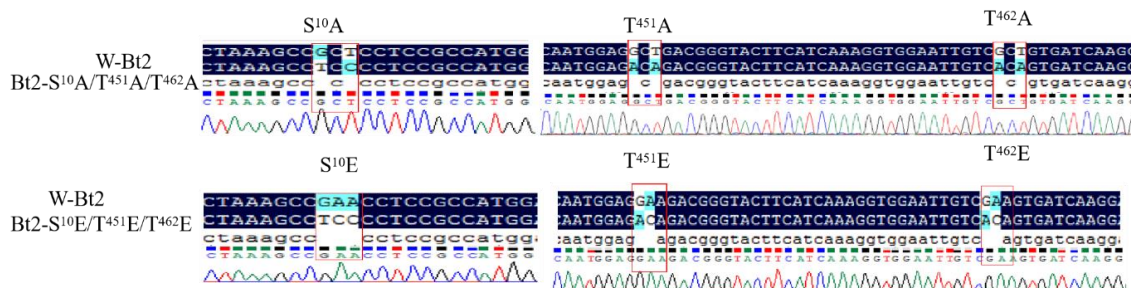


Figure 1. Sequence diagram of site-directed point mutations. W-Bt2 represents the reference Bt2 sequence from the NCBI database. Bt2-S10A/T451A/T462E highlights the sequence region encompassing the serine 10 site replaced with alanine, threonine 451 sites replaced with alanine, and threonine 462 sites replaced with alanine. Bt2-S10E/T451E/T462E highlights the sequence region encompassing the serine 10 site replaced with glutamic acid, threonine 451 sites replaced with glutamic acid, and threonine 462 sites replaced with glutamic acid. White sequence lines demonstrate the primers used for site-directed mutagenesis.

3.3. Mutations Effects on Subcellular Localization of AGPase Small Subunit Bt2

Figure 2 depicts the localization of various mutation types within maize endosperm protoplasts. The subcellular localization of 35S-eGFP served as the control group, while Bt2-eGFP, Bt2-S10/T451/T462A-eGFP, and Bt2-S10/T451/T462E-eGFP constituted the experimental groups. Observations from Figure 1 reveal that both the control and experimental groups displayed signals in the nucleus and cytoplasm. Signals from Bt2-eGFP and Bt2-S10/T451/T462E-eGFP were distributed throughout the entire cell, while those from Bt2-S10/T451/T462A-eGFP were primarily localized around the nucleus. The results demonstrated that the subcellular localization of Bt2 remains unaffected by the mutations.

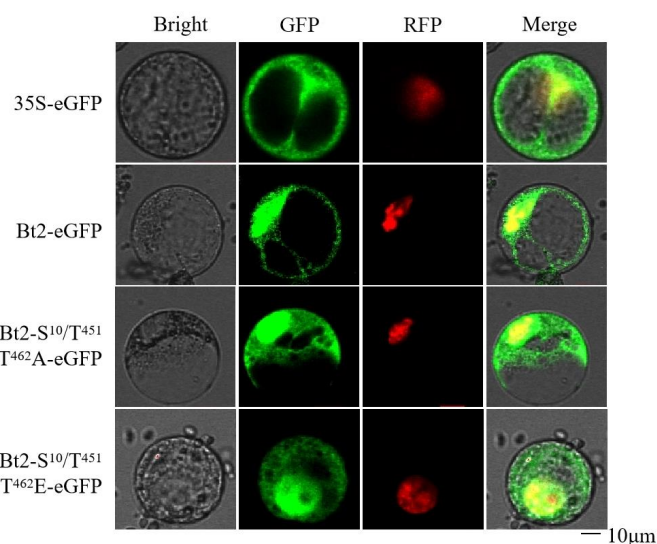


Figure 2. Subcellular localization analysis of Bt2 with phosphorylation site mutations in maize endosperm protoplasts. “Bright” refers to the bright field; the localization signal represents the GFP and the corresponding fusion protein. “RFP” designates the red fluorescence signal indicative of nuclear localization. “Merged” illustrates the composite signal resulting from the superimposition of GFP and RFP (nucleus signals). The mutant’s description is the same as described in Figure 1.

3.4. Interaction between Bt2 with Phosphorylation Sites Mutations and Sh2

We employed yeast two-hybrid assays using the constructed yeast vectors, and the resulting interactions were analyzed. The yeast two-hybrid results are presented in Figure 3. All colonies exhibited normal growth on the second deficient medium, while the negative controls, pGBKT7+pGADT7-Bt2, and pGBKT7+pGADT7, demonstrated impaired growth on the fourth deficient medium. Contrarily, the experimental groups, pGBKT7-Sh2+pGADT7-Bt2, pGBKT7-Sh2+pGADT7-Bt2-S10/T451/T462A, and pGBKT7-Sh2+pGADT7-Bt2-S10/T451/T462E, maintained normal growth on all four deficient mediums. The experimental results indicate that the interaction between the large and small subunits persists, even after site-specific mutations.

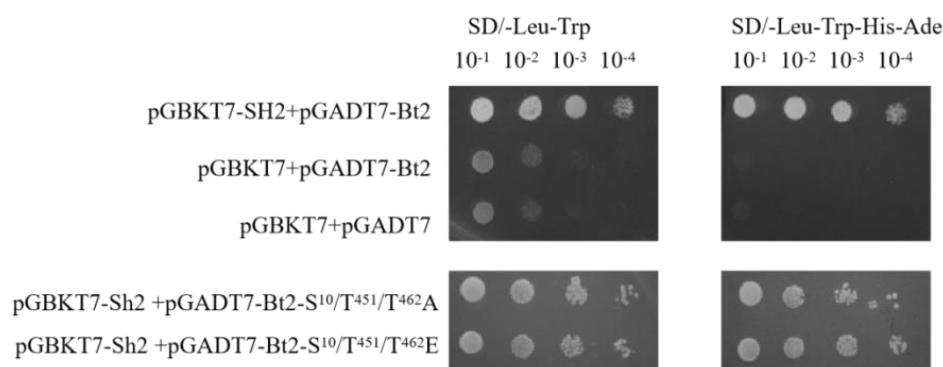


Figure 3. Yeast two-hybrid interaction analysis of Sh2 with mutants. Transformed yeast was plated on SD/−Leu−Trp and SD/−His−Leu−Trp−Ade gradient dilution plates (10^{-1} , 10^{-2} , 10^{-3} , and 10^{-4}). The mutant description is the same as described in Figure 1.

3.5. Bimolecular Fluorescence Complementation Confirms Bt2 Interaction with Sh2

The bimolecular fluorescence complementation (BiFC) experiment was employed to transfect maize leaf protoplasts, aiming to observe the interaction between the Bt2 point mutations and the large subunit Sh2. The findings from this investigation are depicted in Figure 4. In the negative control group, represented by N YFP + C YFP, no YFP fluorescence signal was observed. In contrast, the experimental groups Bt2-S10A-N YFP + Sh2-C YFP, Bt2-S10/T451/T462A-N YFP + Sh2-C YFP, and Bt2-S10/T451/T462E-N YFP + Sh2-C YFP all exhibited a YFP fluorescence signal within the chloroplast. These experimental findings provide evidence that the Bt2 protein retains its interaction with the large subunit Sh2 following point mutation. Importantly, the interaction site was identified within the chloroplast. This substantiates the role of Bt2 and its interactions within the chloroplast even after undergoing point mutations, underpinning the robustness of these biological interactions and their potential role in chloroplast functions.

3.6. Effects of Site-Directed Point Mutations on AGPase Activity

UG221-Sh2 along with various mutant types of UG221-Bt2 were co-transfected into the protoplasts of etiolated seedlings for transient expression. The transfected protoplasts were then cultivated in darkness for 16 h. Subsequently, ATP levels were evaluated using the ATP detection kit provided by Beyotime Biotech, with the experimental findings illustrated in Figure 5. Taking the Bt2 + Sh2 interaction as a baseline, a significant decrease in AGPase activity was observed in the Bt2-S10/T451/T462A + Sh2 measurements. Conversely, the AGPase activity assessed using Bt2-S10/T451/T462E + Sh2 demonstrated an increase. These results provide compelling evidence that point mutations can indeed alter AGPase activity. In this experiment, it was observed that the simulation of dephosphorylation led to a reduction in AGPase activity, whereas the simulation of phosphorylation prompted an increase in AGPase activity. This underscores the profound impact of phosphorylation status on enzymatic function, highlighting the intricate relationship between posttranslational modifications and enzyme activity.

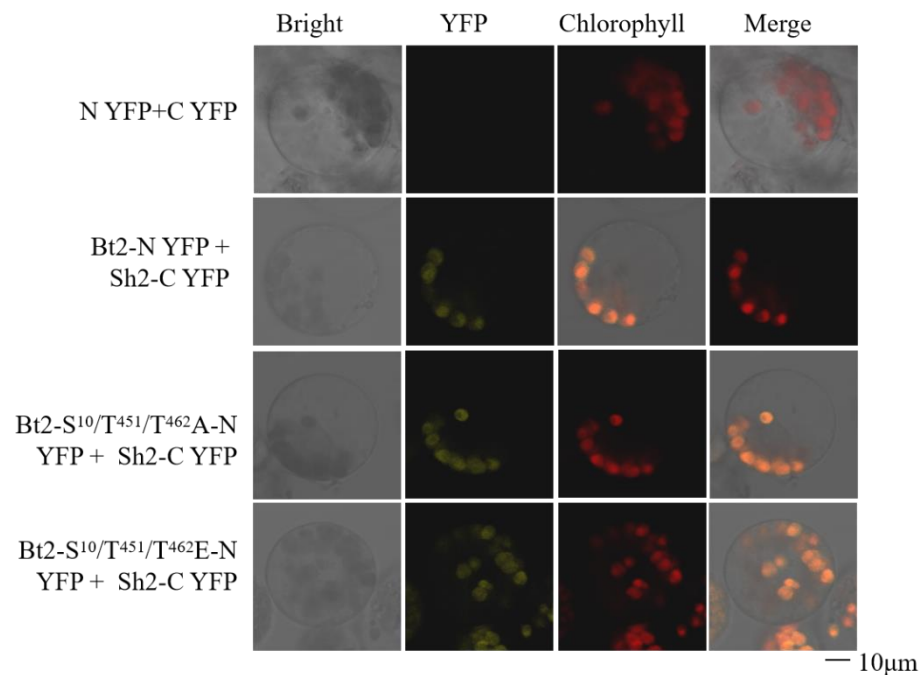


Figure 4. The bimolecular fluorescence complementation between different mutants of Bt2 and Sh2. Fluorescence signals indicate that the Bt2 protein retains its interaction with the large subunit Sh2. The mutant's description is the same as described in Figure 1.

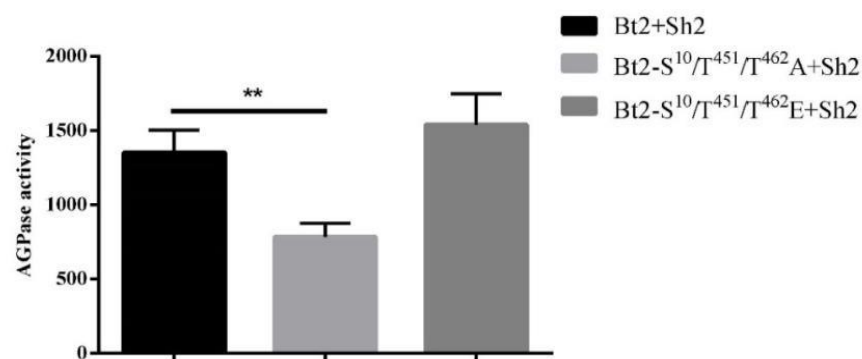


Figure 5. Comparison of AGPase activity between Bt2 with mutated phosphorylation sites and Sh2. The data represent three independent biological replicates (** $p < 0.01$). The mutant's description is the same as described in Figure 1.

4. Discussion

AGPase acts as the key enzyme regulating starch biosynthesis and is indispensable for catalyzing the formation of ADP-Glc from Glc-1-P and ATP [7]. Its operational efficacy is tightly linked to the process of starch synthesis, with any inhibition resulting in a decline in starch output [31,32]. The regulation of AGPase activity is not uniform and varies among different tissues and cells, affecting its overall performance [33–35]. In an adaptive response to fluctuating environmental conditions, the function of AGPase is governed by several regulatory pathways. These encompass redox regulation, allosteric regulation [20], and transcriptional control [21,22] topics that have been subject to extensive research. In cereal endosperm, AGPase activity is primarily derived from the cytoplasm, which also hosts the localization of the small subunit Bt2 examined in this study. However, Bt2 localization is not exclusive to the cytoplasm; it is also found within the nucleus. Previous research reported the localization of the wild-type Bt2 in both the plastid and the cytoplasm [36]. Bt2 exhibits two alternative splices, Bt2a and Bt2b, with Bt2a encoding for cytoplasmic AGPase and being situated within the cytoplasm [37]. However, this past

research primarily investigated just the initial 99 amino acids at the N-terminus. Moreover, previous findings also demonstrated the presence of Bt2-GFP in the maize, with GFP signals noted in both the cytoplasm and nucleus, suggesting the involvement of Bt2 in the regulation of other pathways.

The potential influence of phosphorylation on protein interactions is a significant aspect of this study. In light of our prior research on AGPase activation [26], we suggest that AGPase phosphorylation could be a crucial regulatory mechanism impacting its function. In this experiment, the maize AGPase small subunit Bt2-S10, Bt2-T451, and Bt2-T462 sites underwent mutation to either A or E. Yeast two-hybrid experiments revealed that various mutation types interacted with Sh2. The fluorescence bimolecular complementation experiments further established the presence of protein interactions between different mutation types of Bt2-N YFP and the Sh2-C YFP fusion protein, which were exclusively localized within the chloroplast. This suggests that even after site-specific mutations, the small subunit Bt2 continues to interact with the large subunit Sh2, implying that these mutations do not interfere with the structure of AGPase, allowing for tetramer formation [38]. In summary, our findings contribute to a deeper understanding of the molecular interplay between the Sh2 and Bt2 proteins during maize endosperm development. Moreover, the data imply that Bt2 mutations do not disturb the interaction and potential function of the Sh2–Bt2 protein complex.

Protein phosphorylation has been established to modify protein structure, influencing protein–protein interactions, and thereby affecting these protein functions [39,40]. Such alterations could have implications on protein activity, its intracellular localization, and the stability of complexes it forms with other proteins [6,41]. Research into the phosphorylation of the barley stripe mosaic virus gamma Ser-96-b protein revealed that phosphorylation at crucial sites was vital for protein function [42]. It was discovered that a nonphosphorylated mutant (S96A) of γ B had markedly reduced viral suppressor of RNA silencing (VSR) activity, compared to the phosphorylation-simulated mutant (S96D) and the wild-type γ B, both of which exhibited comparable VSR activities. This study implies that changes induced by phosphorylation can significantly alter protein function. Similarly, an investigation found the phosphorylation status of the tau protein to directly affect its intracellular localization [43]. When phosphorylation was simulated by substituting serine/threonine residues with glutamate in the N-terminal region of the protein, it was observed to impede its membrane localization in transfected cells [26]. Furthermore, it is well established that the phosphorylation of enzymes like SBEI and SP (starch phosphorylase) in maize is crucial for forming active multiprotein complexes [12,44–46]. In addition, studies on wheat endosperm have shown that phosphorylation is necessary for the formation of the SS–SBEII protein complex and the protein complex between SBEIIb and SP [12]. Investigations into the Sh2 gene in maize, which encodes the large subunit of AGPase, suggest that its phosphorylation may affect AGPase activity, localization, and binding [26]. Experiments leveraging the yeast two-hybrid method and bimolecular fluorescence complementation have demonstrated that certain mutations in the Bt2 gene do not impact its interaction with Sh2. Interestingly, the Bt2 mutants, simulating phosphorylation, exhibited increased activity, possibly via a mechanism involving interaction with other proteins or alteration of the enzyme conformation [47] (warranting further investigation). When transiently expressed in endosperm protoplasts, these findings hint at its potential to enhance starch content. Given these findings, future work should aim to validate these results *in vivo* and examine the mechanistic underpinnings of this observed effect. This could involve investigations into the structural changes induced by these mutations, the potential interaction partners of the mutated Sh2 subunit, and the broader impact of these mutations on starch biosynthesis and plant physiology. Such studies will undoubtedly enrich our understanding of the regulatory complexity of AGPase and provide novel avenues for starch improvement. In general, the observed effects of site mutations on AGPase activity suggest the crucial role of these residues' phosphorylation for optimal maize AGPase activity. This study noted an increase in enzyme activity for the co-transformed phosphorylated modified small subunit

and large subunit. In contrast, the enzyme activity for the dephosphorylated modified form was significantly lower than the wild type. The existing literature suggests that the dephosphorylated small subunit Bt2 might cause the active band formed by AGPase to either disappear or decrease, leading to reduced enzymatic activity when the small subunit is fully mutated to A. However, this study focused on the simultaneous mutation of three sites, and the mutation status of individual sites may differ. These insights offer new directions for enhancing AGPase activity following AGPase molecular modification, which hints that phosphorylation at specified site could enhance starch synthesis process.

5. Conclusions

In this study, the point mutation of Bt2, the small subunit, was found not to have an impact on its subcellular location. Bt2 remained localized within the nucleus and the cytoplasm, suggesting that the fundamental cellular distribution of the protein was not perturbed by these point mutations. Furthermore, this point mutation did not appear to hinder Bt2 interaction with its larger counterpart, Sh2. In maize leaf protoplasts, their interaction continued to take place primarily within the chloroplast, maintaining the subcellular site for this crucial protein–protein interaction. Intriguingly, the point mutations of Bt2 had a substantial effect on the activity of the AGPase enzyme, particularly in the context of its phosphorylation state. When the mutated Bt2 was subject to phosphorylation modifications, the activity of AGPase increased, which hints that phosphorylation at the specified site could enhance the starch synthesis process. Conversely, dephosphorylation led to a decrease in AGPase activity, implying that phosphorylation could be a vital regulatory mechanism for the functionality of this enzyme. The nuanced influence of these point mutations on AGPase activity, depending on its phosphorylation status, suggests a critical role for phosphorylation in modulating the enzymatic activity of AGPase. This dynamic could be harnessed to optimize starch synthesis in crop production, an area that warrants further investigation. Through the creation and examination of mutants with augmented AGPase activity, this research sets the stage for the possible creation of crop variations with superior starch content. Such advancements could enhance both crop yield and quality. Additionally, comprehension of the way the phosphorylation status of Sh2 affects AGPase activity may lead to the cultivation of crop variations with altered starch characteristics, potentially amplifying their utility across various industries, such as the food, pharmaceutical, and biofuel sectors.

Supplementary Materials: The following supporting information can be downloaded at: <https://www.mdpi.com/article/10.3390/agronomy13082119/s1>, Table S1: List of Primers used in this experiment.

Author Contributions: G.Y. and Y.H. designed the experiments and wrote the article. N.S. and Y.Y. analyzed the subcellular localization and activity of Bt2 and performed yeast two-hybrid assays. G.Y., Y.Y. and L.L. performed the phosphorylation site analysis. N.S., N.M. and Y.M. analyzed the activity of AGPase. All authors have read and agreed to the published version of the manuscript.

Funding: This work was supported by the China Agriculture Research System (CARS-05), the Natural Science Foundation of China (No: 31501322 and 31971960), Postdoctoral Special Foundation of Sichuan Province (No: 03130104), and the Overseas Scholar Science and Technology Activities Project Merit Funding (No: 00124300).

Institutional Review Board Statement: Not applicable for studies not involving humans or animals.

Informed Consent Statement: Not applicable.

Data Availability Statement: Not applicable.

Acknowledgments: We would like to thank Wang Bai and Jianglin Xiang for their technical support. This work was partly supported by the College of Agronomy, Sichuan Agricultural University.

Conflicts of Interest: The authors declare that this research was conducted in the absence of any commercial or financial relationships that could be construed as a potential conflict of interest.

References

1. Myburgh, J.A.; Finfer, S.; Bellomo, R.; Billot, L.; Cass, A.; Gattas, D.; Glass, P.; Lipman, J.; Liu, B.; McArthur, C. Hydroxyethyl starch or saline for fluid resuscitation in intensive care. *N. Engl. J. Med.* **2012**, *367*, 1901–1911. [[CrossRef](#)]
2. Mojović, L.; Pejin, D.; Grujić, O.; Markov, S.; Pejin, J.; Rakin, M.; Vukašinović, M.; Nikolić, S.; Savić, D. Progress in the production of bioethanol on starch-based feedstocks. *Chem. Ind. Chem. Eng. Q.* **2009**, *15*, 211–226. [[CrossRef](#)]
3. Asharuddin, S.M.; Othman, N.; Altowayti, W.A.H.; Bakar, N.A.; Hassan, A. Recent advancement in starch modification and its application as water treatment agent. *Environ. Technol. Innov.* **2021**, *23*, 101637. [[CrossRef](#)]
4. Wang, Q.; Chen, Y. Advantages Analysis of Corn Planting in China. *J. Agric. Sci. Technol. China* **2018**, *20*, 1–9.
5. Willett, J. Starch in polymer compositions. In *Starch*; Elsevier: Amsterdam, The Netherlands, 2009; pp. 715–743.
6. Shoaib, N.; Liu, L.; Ali, A.; Mughal, N.; Yu, G.; Huang, Y. Molecular Functions and Pathways of Plastidial Starch Phosphorylase (PHO1) in Starch Metabolism: Current and Future Perspectives. *Int. J. Mol. Sci.* **2021**, *22*, 10450. [[CrossRef](#)] [[PubMed](#)]
7. Boehlein, S.K.; Shaw, J.R.; Stewart, J.D.; Hannah, L.C. Studies of the kinetic mechanism of maize endosperm ADP-glucose pyrophosphorylase uncovered complex regulatory properties. *Plant Physiol.* **2010**, *152*, 1056–1064. [[CrossRef](#)]
8. Crofts, N.; Sugimoto, K.; Oitome, N.F.; Nakamura, Y.; Fujita, N. Differences in specificity and compensatory functions among three major starch synthases determine the structure of amylopectin in rice endosperm. *Plant Mol. Biol.* **2017**, *94*, 399–417. [[CrossRef](#)] [[PubMed](#)]
9. Tickle, P.; Burrell, M.M.; Coates, S.A.; Emes, M.J.; Tetlow, I.J.; Bowsher, C.G. Characterization of plastidial starch phosphorylase in *Triticum aestivum* L. endosperm. *J. Plant Physiol.* **2009**, *166*, 1465–1478. [[CrossRef](#)] [[PubMed](#)]
10. Satoh, H.; Shibahara, K.; Tokunaga, T.; Nishi, A.; Tasaki, M.; Hwang, S.K.; Okita, T.W.; Kaneko, N.; Fujita, N.; Yoshida, M.; et al. Mutation of the plastidial alpha-glucan phosphorylase gene in rice affects the synthesis and structure of starch in the endosperm. *Plant Cell* **2008**, *20*, 1833–1849. [[CrossRef](#)]
11. Grimaud, F.; Rogniaux, H.; James, M.G.; Myers, A.M.; Planchot, V. Proteome and phosphoproteome analysis of starch granule-associated proteins from normal maize and mutants affected in starch biosynthesis. *J. Exp. Bot.* **2008**, *59*, 3395–3406. [[CrossRef](#)]
12. Tetlow, I.J.; Beisel, K.G.; Cameron, S.; Makhmoudova, A.; Liu, F.; Bresolin, N.S.; Wait, R.; Morell, M.K.; Emes, M.J. Analysis of protein complexes in wheat amyloplasts reveals functional interactions among starch biosynthetic enzymes. *Plant Physiol.* **2008**, *146*, 1878–1891. [[CrossRef](#)]
13. Hannah, L.C.; Shaw, J.R.; Giroux, M.J.; Reyss, A.; Prioul, J.-L.; Bae, J.-M.; Lee, J.-Y. Maize genes encoding the small subunit of ADP-glucose pyrophosphorylase. *Plant Physiol.* **2001**, *127*, 173–183. [[CrossRef](#)]
14. Corbi, J.; Debieu, M.; Rousselet, A.; Montalent, P.; Le Guilloux, M.; Manicacci, D.; Tenailon, M. Contrasted patterns of selection since maize domestication on duplicated genes encoding a starch pathway enzyme. *Theor. Appl. Genet.* **2011**, *122*, 705–722. [[CrossRef](#)]
15. Cakir, B.; Tuncel, A.; Green, A.R.; Koper, K.; Hwang, S.-K.; Okita, T.W.; Kang, C. Substrate binding properties of potato tuber ADP-glucose pyrophosphorylase as determined by isothermal titration calorimetry. *FEBS Lett.* **2015**, *589*, 1444–1449. [[CrossRef](#)] [[PubMed](#)]
16. Comparot-Moss, S.; Denyer, K. The evolution of the starch biosynthetic pathway in cereals and other grasses. *J. Exp. Bot.* **2009**, *60*, 2481–2492. [[CrossRef](#)]
17. Bowsher, C.G.; Scrase-Field, E.F.; Esposito, S.; Emes, M.J.; Tetlow, I.J. Characterization of ADP-glucose transport across the cereal endosperm amyloplast envelope. *J. Exp. Bot.* **2007**, *58*, 1321–1332. [[CrossRef](#)]
18. Kirchberger, S.; Leroch, M.; Huynen, M.A.; Wahl, M.; Neuhaus, H.E.; Tjaden, J. Molecular and biochemical analysis of the plastidic ADP-glucose transporter (ZmBT1) from *Zea mays*. *J. Biol. Chem.* **2007**, *282*, 22481–22491. [[CrossRef](#)] [[PubMed](#)]
19. Tuncel, A. *Allosteric Regulation of the Rice Endosperm ADP-Glucose Pyrophosphorylase*; Washington State University: Washington, DC, USA, 2013.
20. Geigenberger, P. Regulation of sucrose to starch conversion in growing potato tubers. *J. Exp. Bot.* **2003**, *54*, 457–465. [[CrossRef](#)] [[PubMed](#)]
21. Mangelsen, E.; Wanke, D.; Kilian, J.; Sundberg, E.; Harter, K.; Jansson, C. Significance of light, sugar, and amino acid supply for diurnal gene regulation in developing barley caryopses. *Plant Physiol.* **2010**, *153*, 14–33. [[CrossRef](#)] [[PubMed](#)]
22. Smith, S.M.; Fulton, D.C.; Chia, T.; Thorneycroft, D.; Chapple, A.; Dunstan, H.; Hylton, C.; Zeeman, S.C.; Smith, A.M. Diurnal changes in the transcriptome encoding enzymes of starch metabolism provide evidence for both transcriptional and posttranscriptional regulation of starch metabolism in Arabidopsis leaves. *Plant Physiol.* **2004**, *136*, 2687–2699. [[CrossRef](#)] [[PubMed](#)]
23. Nakagami, H.; Sugiyama, N.; Mochida, K.; Daudi, A.; Yoshida, Y.; Toyoda, T.; Tomita, M.; Ishihama, Y.; Shirasu, K. Large-scale comparative phosphoproteomics identifies conserved phosphorylation sites in plants. *Plant Physiol.* **2010**, *153*, 1161–1174. [[CrossRef](#)]
24. Rose, C.M.; Venkateshwaran, M.; Volkening, J.D.; Grimsrud, P.A.; Maeda, J.; Bailey, D.J.; Park, K.; Howes-Podoll, M.; den Os, D.; Yeun, L.H. Rapid phosphoproteomic and transcriptomic changes in the rhizobia-legume symbiosis. *Mol. Cell. Proteom.* **2012**, *11*, 724–744. [[CrossRef](#)] [[PubMed](#)]
25. Dong, K.; Zhen, S.; Cheng, Z.; Cao, H.; Ge, P.; Yan, Y. Proteomic analysis reveals key proteins and phosphoproteins upon seed germination of wheat (*Triticum aestivum* L.). *Front. Plant Sci.* **2015**, *6*, 1017. [[CrossRef](#)] [[PubMed](#)]

26. Yu, G.; Lv, Y.; Shen, L.; Wang, Y.; Qing, Y.; Wu, N.; Li, Y.; Huang, H.; Zhang, N.; Liu, Y.; et al. The Proteomic Analysis of Maize Endosperm Protein Enriched by Phos-tag(tm) Reveals the Phosphorylation of Brittle-2 Subunit of ADP-Glc Pyrophosphorylase in Starch Biosynthesis Process. *Int. J. Mol. Sci.* **2019**, *20*, 986. [[CrossRef](#)]
27. Ferrero, D.M.; Piattoni, C.V.; Asencio Diez, M.D.; Rojas, B.E.; Hartman, M.D.; Ballicora, M.A.; Iglesias, A.A. Phosphorylation of ADP-glucose pyrophosphorylase during wheat seeds development. *Front. Plant Sci.* **2020**, *11*, 1058. [[CrossRef](#)] [[PubMed](#)]
28. Wiese, S.; Reidegeld, K.A.; Meyer, H.E.; Warscheid, B. Protein labeling by iTRAQ: A new tool for quantitative mass spectrometry in proteome research. *Proteomics* **2007**, *7*, 340–350. [[CrossRef](#)] [[PubMed](#)]
29. Yokoe, H.; Meyer, T. Spatial dynamics of GFP-tagged proteins investigated by local fluorescence enhancement. *Nat. Biotechnol.* **1996**, *14*, 1252–1256. [[CrossRef](#)]
30. Paiano, A.; Margiotta, A.; De Luca, M.; Bucci, C. Yeast two-hybrid assay to identify interacting proteins. *Curr. Protoc. Protein Sci.* **2019**, *95*, e70. [[CrossRef](#)] [[PubMed](#)]
31. Bahaji, A.; Li, J.; Sánchez-López, Á.M.; Baroja-Fernández, E.; Muñoz, F.J.; Ovecka, M.; Almagro, G.; Montero, M.; Ezquer, I.; Etxeberria, E. Starch biosynthesis, its regulation and biotechnological approaches to improve crop yields. *Biotechnol. Adv.* **2014**, *32*, 87–106. [[CrossRef](#)]
32. Cross, J.M.; Clancy, M.; Shaw, J.R.; Greene, T.W.; Schmidt, R.R.; Okita, T.W.; Hannah, L.C. Both subunits of ADP-glucose pyrophosphorylase are regulatory. *Plant Physiol.* **2004**, *135*, 137–144. [[CrossRef](#)]
33. Greene, T.W.; Hannah, L.C. Enhanced stability of maize endosperm ADP-glucose pyrophosphorylase is gained through mutants that alter subunit interactions. *Proc. Natl. Acad. Sci. USA* **1998**, *95*, 13342–13347. [[CrossRef](#)] [[PubMed](#)]
34. Li, N.; Zhang, S.; Zhao, Y.; Li, B.; Zhang, J. Over-expression of AGPase genes enhances seed weight and starch content in transgenic maize. *Planta* **2011**, *233*, 241–250. [[CrossRef](#)]
35. Stark, D.M.; Timmerman, K.P.; Barry, G.F.; Preiss, J.; Kishore, G.M. Regulation of the amount of starch in plant tissues by ADP glucose pyrophosphorylase. *Science* **1992**, *258*, 287–292. [[CrossRef](#)] [[PubMed](#)]
36. Lee, S.-K.; Hwang, S.-K.; Han, M.; Eom, J.-S.; Kang, H.-G.; Han, Y.; Choi, S.-B.; Cho, M.-H.; Bhoo, S.H.; An, G. Identification of the ADP-glucose pyrophosphorylase isoforms essential for starch synthesis in the leaf and seed endosperm of rice (*Oryza sativa* L.). *Plant Mol. Biol.* **2007**, *65*, 531–546. [[CrossRef](#)]
37. Rogowsky, P. *Transcriptional and Metabolic Adjustments in AGPase Deficient bt2 Maize Kernels*; American Society of Plant Biologists: Rockville, MD, USA, 2008.
38. Koper, K. Glutamic Acid 358 Is Important for the Normal Allosteric Function and Heterotetramer Formation of Potato Adp-Glucose Pyrophosphorylase. Master's Thesis, Fen Bilimleri Enstitüsü, Ankara, Turkey, 2013.
39. Cohen, P. The regulation of protein function by multisite phosphorylation—A 25 year update. *Trends Biochem. Sci.* **2000**, *25*, 596–601. [[CrossRef](#)]
40. Pysh, L.D.; Aukerman, M.J.; Schmidt, R.J. OHP1: A maize basic domain/leucine zipper protein that interacts with opaque2. *Plant Cell* **1993**, *5*, 227–236. [[PubMed](#)]
41. Liu, X.; Wang, Z.; Wang, L.; Wu, R.; Phillips, J.; Deng, X. LEA 4 group genes from the resurrection plant *Boea hygrometrica* confer dehydration tolerance in transgenic tobacco. *Plant Sci.* **2009**, *176*, 90–98. [[CrossRef](#)]
42. Zhang, X.; Dong, K.; Xu, K.; Zhang, K.; Jin, X.; Yang, M.; Zhang, Y.; Wang, X.; Han, C.; Yu, J. Barley stripe mosaic virus infection requires PKA-mediated phosphorylation of γ b for suppression of both RNA silencing and the host cell death response. *New Phytol.* **2018**, *218*, 1570–1585. [[CrossRef](#)]
43. Pooler, A.M.; Usardi, A.; Evans, C.J.; Philpott, K.L.; Noble, W.; Hanger, D.P. Dynamic association of tau with neuronal membranes is regulated by phosphorylation. *Neurobiol. Aging* **2012**, *33*, 431.e27–431.e38. [[CrossRef](#)]
44. Tetlow, I.J.; Wait, R.; Lu, Z.; Akkasaeng, R.; Bowsher, C.G.; Esposito, S.; Kosar-Hashemi, B.; Morell, M.K.; Emes, M.J. Protein phosphorylation in amyloplasts regulates starch branching enzyme activity and protein-protein interactions. *Plant Cell* **2004**, *16*, 694–708. [[CrossRef](#)]
45. Yu, G.; Shoaib, N.; Xie, Y.; Liu, L.; Mughal, N.; Li, Y.; Huang, H.; Zhang, N.; Zhang, J.; Liu, Y. Comparative Study of Starch Phosphorylase Genes and Encoded Proteins in Various Monocots and Dicots with Emphasis on Maize. *Int. J. Mol. Sci.* **2022**, *23*, 4518. [[CrossRef](#)] [[PubMed](#)]
46. Yu, G.; Gaoyang, Y.; Liu, L.; Shoaib, N.; Deng, Y.; Zhang, N.; Li, Y.; Huang, Y. The Structure, Function, and Regulation of Starch Synthesis Enzymes SSIII with Emphasis on Maize. *Agronomy* **2022**, *12*, 1359. [[CrossRef](#)]
47. Figueroa, C.M.; Asencio Diez, M.D.; Ballicora, M.A.; Iglesias, A.A. Structure, function, and evolution of plant ADP-glucose pyrophosphorylase. *Plant Mol. Biol.* **2022**, *108*, 307–323. [[CrossRef](#)] [[PubMed](#)]

Disclaimer/Publisher's Note: The statements, opinions and data contained in all publications are solely those of the individual author(s) and contributor(s) and not of MDPI and/or the editor(s). MDPI and/or the editor(s) disclaim responsibility for any injury to people or property resulting from any ideas, methods, instructions or products referred to in the content.